Diabetologia (2019) 62:123–135
https://doi.org/10.1007/s00125-018-4746-4

ARTICLE

Pleiotrophin deletion alters glucose homeostasis, energy metabolism and brown fat thermogenic function in mice

Julio Sevillano[1] · María Gracia Sánchez-Alonso[1] · Begoña Zapatería[1] · María Calderón[1] · Martín Alcalá[1] · María Limones[1] · Jimena Pita[1] · Esther Gramage[2] · Marta Vicente-Rodríguez[2] · Daniel Horrillo[3] · Gema Medina-Gómez[3] · María Jesús Obregón[4] · Marta Viana[1] · Ismael Valladolid-Acebes[5] · Gonzalo Herradón[2] · María Pilar Ramos-Álvarez[1]

Received: 30 June 2018 / Accepted: 22 August 2018 / Published online: 16 October 2018

Abstract

Aims/hypothesis Pleiotrophin, a developmentally regulated and highly conserved cytokine, exerts different functions including regulation of cell growth and survival. Here, we hypothesise that this cytokine can play a regulatory role in glucose and lipid homeostasis.

Methods To test this hypothesis, we performed a longitudinal study characterising the metabolic profile (circulating variables and tissue mRNA expression) of gene-targeted *Ptn*-deficient female mice and their corresponding wild-type counterparts at different ages from young adulthood (3 months) to older age (15 months). Metabolic cages were used to investigate the respiratory exchange ratio and energy expenditure, at both 24°C and 30°C. Undifferentiated immortalised mouse brown adipocytes (mBAs) were treated with 0.1 μg/ml pleiotrophin until day 6 of differentiation, and markers of mBA differentiation were analysed by quantitative real-time PCR (qPCR).

Results *Ptn* deletion was associated with a reduction in total body fat (20.2% in $Ptn^{+/+}$ vs 13.9% in $Ptn^{-/-}$ mice) and an enhanced lipolytic response to isoprenaline in isolated adipocytes from 15-month-old mice (189% in $Ptn^{+/+}$ vs 273% in $Ptn^{-/-}$ mice). We found that $Ptn^{-/-}$ mice exhibited a significantly lower QUICKI value and an altered lipid profile; plasma triacylglycerols and NEFA did not increase with age, as happens in $Ptn^{+/+}$ mice. Furthermore, the contribution of cold-induced thermogenesis to energy expenditure was greater in $Ptn^{-/-}$ than $Ptn^{+/+}$ mice (42.6% and 33.6%, respectively). Body temperature and the activity and expression of deiodinase, T_3 and mitochondrial uncoupling protein-1 in the brown adipose tissue of $Ptn^{-/-}$ mice were higher than in wild-type controls. Finally, supplementing brown pre-adipocytes with pleiotrophin decreased the expression of the brown adipocyte markers *Cidea* (20% reduction), *Prdm16* (21% reduction), and *Pgc1-α* (also known as *Ppargc1a*, 11% reduction).

Conclusions/interpretation Our results reveal for the first time that pleiotrophin is a key player in preserving insulin sensitivity, driving the dynamics of adipose tissue lipid turnover and plasticity, and regulating energy metabolism and thermogenesis. These findings open therapeutic avenues for the treatment of metabolic disorders by targeting pleiotrophin in the crosstalk between white and brown adipose tissue.

Keywords Adipose tissue · Glucose homeostasis · Insulin resistance · Metabolism · Pleiotrophin · Thermogenesis

Julio Sevillano and María Gracia Sánchez-Alonso are joint first authors.

✉ María Pilar Ramos-Álvarez
pramos@ceu.es

[1] Department of Chemistry and Biochemistry, Facultad de Farmacia, Universidad CEU San Pablo, Ctra. Boadilla del Monte km 5,3, 28668 Madrid, Spain

[2] Department of Pharmaceutical and Health Sciences, Facultad de Farmacia, Universidad CEU San Pablo, Madrid, Spain

[3] Department of Basic Sciences of Health, Universidad Rey Juan Carlos, Alcorcón, Madrid, Spain

[4] Department of Endocrine and Nervous System Pathophysiology, Instituto de Investigaciones Biomédicas 'Alberto Sols', Consejo Superior de Investigaciones Científicas (CSIC)-Universidad Autónoma de Madrid (UAM), Madrid, Spain

[5] The Rolf Luft Research Center for Diabetes and Endocrinology, Department of Molecular Medicine and Surgery, Karolinska Institutet, Stockholm, Sweden

Research in context

What is already known about this subject?

- Pleiotrophin signalling may be involved in the inhibition of white pre-adipocyte differentiation in vitro

What is the key question?

- Is pleiotrophin a modulator of lipid and glucose homeostasis, regulating fat accumulation, body composition and thermogenic function of brown fat?

What are the new findings?

- Pleiotrophin deficiency ameliorates insulin sensitivity in older mice and is associated with an altered expansibility of periovarian adipose tissue as well as with enhanced cell differentiation and thermogenesis of brown adipose tissue
- The impaired lipid and glucose homeostasis in *Ptn*-deficient mice could be attributed to defective PPAR-γ activation

How might this impact on clinical practice in the foreseeable future?

- This study opens therapeutic avenues for the treatment of metabolic disorders by targeting pleiotrophin in the crosstalk between white and brown adipose tissue

Abbreviations

BAT	Brown adipose tissue
DIO2	Deiodinase 2
EC_{50}	Half-maximal effective agonist concentration
EE	Energy expenditure
E_{max}	Maximum effect
GTT	Glucose tolerance test
mBA	Mouse brown adipocyte
I_{max}	Maximum inhibitory effect
PPAR	Peroxisome proliferator-activated receptor
PTN	Pleiotrophin
qPCR	Quantitative real-time PCR
RER	Respiratory exchange ratio
rPTN	Recombinant pleiotrophin
UCP-1	Uncoupling protein-1
$\dot{V}CO_2$	Carbon dioxide production
$\dot{V}O_2$	Oxygen consumption

Introduction

Pleiotrophin (PTN) is a highly conserved cytokine that belongs to a family of heparin-binding growth factors [1, 2]. PTN is found in cells in the early stages of differentiation, in particular during embryonic development [3, 4]. PTN contributes to epithelial–mesenchymal interactions in organs undergoing branching morphogenesis [5–7] and participates in bone formation [8].

In adult rodents, residual *Ptn* expression is restricted to uterine cells and discrete populations in the nervous system [9]. An almost identical expression profile has been found in human adult tissues [10]. PTN levels are, however, upregulated in the uterus and placenta during pregnancy [9], and in the early stages of differentiation of cell types involved in repair [11, 12] and inflammatory processes [13].

Besides its role in tumour growth, the functions of PTN include regulation of cell growth, migration and survival [14]. Importantly, PTN signalling may have an inhibitory role in the differentiation of pre-adipocytes in vitro [15], which involves crosstalk between the PTN/phosphoinositide 3-kinase (PI_3K)/Akt/glycogen synthase kinase (GSK)-3β/β-catenin and Wnt/β-catenin signalling pathways to repress adipogenesis [16]. Upon induction of white adipocyte differentiation, levels of endogenous PTN decrease [17], and the in vitro administration of recombinant PTN (rPTN) inhibits white adipocyte differentiation, leading to a decreased expression of white adipocyte markers such as *Ppar-γ*$_2$ (also known as *Pparg2*) [16, 17].

Our hypothesis proposes a role for PTN as a modulator of lipid and glucose homeostasis that might be involved in fat accumulation and body composition due to specific actions on adipose tissue. To address this question, we phenotyped a whole-body constitutive *Ptn* knockout mouse model ($Ptn^{-/-}$) at different stages of adult life.

Methods

Animals PTN genetically deficient ($Ptn^{-/-}$) mice on a C57BL/6 J background were kindly provided by T. F. Deuel (The Scripps Research Institute, La Jolla, CA, USA) [18, 19]. Female $Ptn^{-/-}$ and wild-type ($Ptn^{+/+}$) mice were housed at 22–24°C with 12 h/12 h light/dark cycles of 08:00/20:00 hours and free access to water and a chow diet (Panlab, Barcelona, Spain). Animals were maintained in accordance with European Union Laboratory Animal Care Rules (86/609/

ECC directive) and protocols approved by the Animal Research Committee of CEU San Pablo University. At 3, 6, 12 and 15 months of age, randomly selected mice from each genotype were fasted for 5 h, exposed to carbon dioxide and killed by decapitation. Researchers and animal caretakers were blinded to group assignment. Plasma and organs were collected and preserved at −80°C.

Determination of body fat Total body fat was extracted from dried cadavers of 6-month-old mice in an automatic Soxhlet extraction system (Buchi extraction system B-811, Flawil, Switzerland) using chloroform–methanol (3:1, vol./vol.).

Plasma analysis, estimation of insulin resistance and GTT Glucose (using the glucose oxidase–peroxidase, aminoantipyrine, phenol method [GOD-PAP]; Roche Diagnostics, Barcelona, Spain), triacylglycerols (using lipoprotein lipase [LPL]/glycerol phosphate oxydase [GPO]/-Trinder; Roche Diagnostics) and NEFA (Acyl-CoA synthase–Acyl-CoA oxidase [ACS-ACOD] method; Wako Chemicals, Neuss, Germany) were determined by enzymatic colorimetric tests. Plasma insulin measurement (Mercodia, Uppsala, Sweden) and free T_4 levels (DRG, NJ, USA) were determined using immunoassay kits. Plasma leptin was measured with a Bio-Plex Pro mouse diabetes immunoassay kit (Bio-Rad, Hercules, CA, USA). The QUICKI insulin sensitivity index was calculated as the inverse log sum of fasting insulin (in pmol/l) and fasting glucose (in mmol/l), as previously described [20]. Glucose tolerance tests (GTTs) using intraperitoneal glucose administration (2 g/kg) were performed in mice that had been fasted for 6 h; AUCs for glucose were calculated.

Quantitative real-time PCR in white adipose tissue RNA was isolated using RNeasy Mini Kits (Qiagen, Valencia, CA, USA). First-strand cDNAs were synthesised using the iScript cDNA Synthesis Kit (Bio-Rad) and subjected to quantitative real-time PCR (qPCR) analysis by SYBR green method (Bio-Rad) in a CFX96 real-time system (Bio-Rad); the primer sequences are shown in Table 1. The relative expression of each gene was normalised against *Hprt* and *Rpl13*, used as reference standards.

Histological studies Randomly selected samples of periovarian adipose tissue were stained with haematoxylin and eosin and analysed by optical microscopy.

Lipolysis analysis in isolated adipocytes Adipocytes were isolated from the periovarian adipose tissue of 15-month-old mice as previously described [21]. To test catecholamine-stimulated lipolysis, isolated adipocytes were incubated with 1 U/ml of adenosine deaminase (Sigma-Aldrich, Madrid, Spain) in the absence or presence of isoprenaline (Sigma-Aldrich). Lipolysis was quantified as liberation of glycerol into the medium, determined by the GPO-Trinder method (Sigma-Aldrich). Basal lipolysis, half-maximal effective agonist concentration (EC_{50}) and maximum effect (E_{max}) for lipolysis were estimated from the concentration vs effect curves of glycerol. To measure the effect of insulin on lipolysis, isolated adipocytes were incubated with 0, 1, 10 or 100 nmol/l insulin (Sigma-Aldrich) prior to the addition of isoprenaline (100 nmol/l) and incubated for 90 min. The IC_{50} and maximum inhibitory effect (I_{max}) values were estimated.

Indirect calorimetry Six-month-old $Ptn^{+/+}$ and $Ptn^{-/-}$ mice were randomly selected and individually housed in chambers at 22–24°C with free access to chow and water. After adaptation for 72 h, the mice were housed for 3 days at 24°C, and then 7 days at 30°C. Oxygen consumption ($\dot{V}O_2$) and carbon dioxide production ($\dot{V}CO_2$) of individual mice were measured every 30 min over 24 h in LabMaster metabolic cages (TSE Systems, Bad Homburg, Germany). Respiratory exchange ratios (RERs) were calculated as $\dot{V}CO_2/\dot{V}O_2$. Data on total

Table 1 Primer sets used for qPCR analysis

Gene	Primer
Rpl13	5′-GGTGCCCTACAGTTAGATACCAC-3′ 5′-TTTGTTTCGCCTCCTTGGGTC-3′
Hprt	5′-TGCTCGAGATGTCATGAAGG-3′ 5′-TATGTCCCCCGTTGACTGAT-3′
Lpl	5′-TGGAGAAGCCATCCGTGTG-3′ 5′-TCATGCGAGCACTTCACCAG-3′
Glut-4	5′-GGAAGGAAAAGGGCTATGCTG-3′ 5′-TGAGGAACCGTCCAAGAATGA-3′
Ucp-2	5′-ACAGCCTTCTGCACTCCTG-3′ 5′-GGCTGGGAGACGAAACACT-3′
Ppar-γ1	5′-TTTAAAAACAAGACTACCCTTTACTG AAATT-3′ 5′-AGAGGTCCACAGAGCTGATTCC-3′
Ppar-γ2	5′-GATGCACTGCCTATGAGCACTT-3′ 5′-AGAGGTCCACAGAGCTGATTCC-3′
Tnf-α	5′-AGGCACTCCCCCAAAAGATG-3′ 5′-TGAGGGTCTGGGCCATAGAA-3′
Adr-β₃	5′-CCGTCGTCTTCTGTGTAGCT-3′ 5′-GCGCACCTTCATAGCCATC-3′
Ctp1α	5′-CCTGGTCCACAGGAAGACAT-3′ 5′-CAATGCGAGCCACAGACTTA-3′
Pgc1-α	5′-GAAAGGGCCAAACAGAGAGA-3′ 5′-GTAAATCACACGGCGCTCTT-3′
Cidea	5′-GCCTGCAGGAACTTATCAGC-3′ 5′-AGAACTCCTCTGTGTCCACCA-3′
Prdm16	5′-CCTAAGGTGTGCCCAGCA-3′ 5′-CACCTTCCGCTTTTCTACCC-3′

The SYBR green qPCR method was used for the gene studies, with the primer sets shown (forward [above] and reverse [below]). The relative expression of each gene was normalised against *Hprt* and *Rpl13*, used as reference standards

energy expenditure (EE) were used to calculate cold-induced thermogenesis as a fraction of total daily EE [22].

Analysis in brown adipose tissue Total T_3 and T_4 concentrations were determined in brown adipose tissue (BAT) from 6-month-old mice by radioimmunoassay [23]. Deiodinase 2 (DIO2) activity was assayed in BAT homogenates as previously described [24]. Mouse *Dio2* mRNA was quantified by qPCR using specific Taqman probes for murine *Dio2* (Applied Biosystems, Foster City, CA, USA). The results were normalised to cyclophilin. Production of uncoupling protein 1 (UCP-1) was determined by Western blotting, using a 1/1000 dilution of a specific rabbit anti-UCP1 antibody validated for western Blot (ab1426, Chemicon, Temecula, CA, USA), the corresponding 1/20000 dilution of a rabbit secondary horse radish peroxidase antibody (A0545, Sigma-Aldrich) and visualisation by enhanced chemiluminescence (Amersham-GE Healthcare, Barcelona, Spain); values were normalised to β-actin using a 1/100 dilution of a specific rabbit anti-β-actin (A2066, Sigma-Aldrich).

Cell culture and differentiation of brown adipocytes Immortalised mBAs were generated as previously described [25], grown in DMEM, supplemented with 10% (vol./vol.) fetal serum, 1% (vol./vol.) penicillin/streptomycin (Sigma-Aldrich) and 2 mmol/l HEPES, and differentiated until they exhibited numerous multilocular cytoplasmic lipid droplets [26]. Undifferentiated (day 0) pre-adipocytes were treated with 0.1 μg/ml PTN (Sigma-Aldrich) until day 6 of differentiation; at this time point, non-treated pre-adipocytes typically achieved a fully differentiated phenotype. Markers of mBA differentiation (*Cidea*, *Pgc1-α* [also known as *Ppargc1a*] and *Prdm16*) and *Ptn* mRNA levels were measured by qPCR (Table 1).

Statistical analysis Results are expressed as mean ± SEM. When data were not normally distributed, $\log_{10}$-transformed values were used for statistical analysis, and a Grubbs' test was run to detect outliers. Statistical comparisons between two groups were made using the unpaired Student's *t* test; comparisons between three or more groups were made by one- or two-way ANOVA, followed by a Student–Newman–Keuls post hoc test, using GraphPad Prism v7 (San Diego, CA, USA).

Results

***Ptn*$^{-/-}$ mice show reduced body weight and adiposity** The survival rate was similar in both genotypes (Fig. 1a). We first investigated whether *Ptn* deletion would affect body weight and fat distribution. The body weight of *Ptn*$^{-/-}$ mice was significantly lower over the whole time course of the study (Fig. 1b). Furthermore, we found that the weights (Fig. 1c, d) of

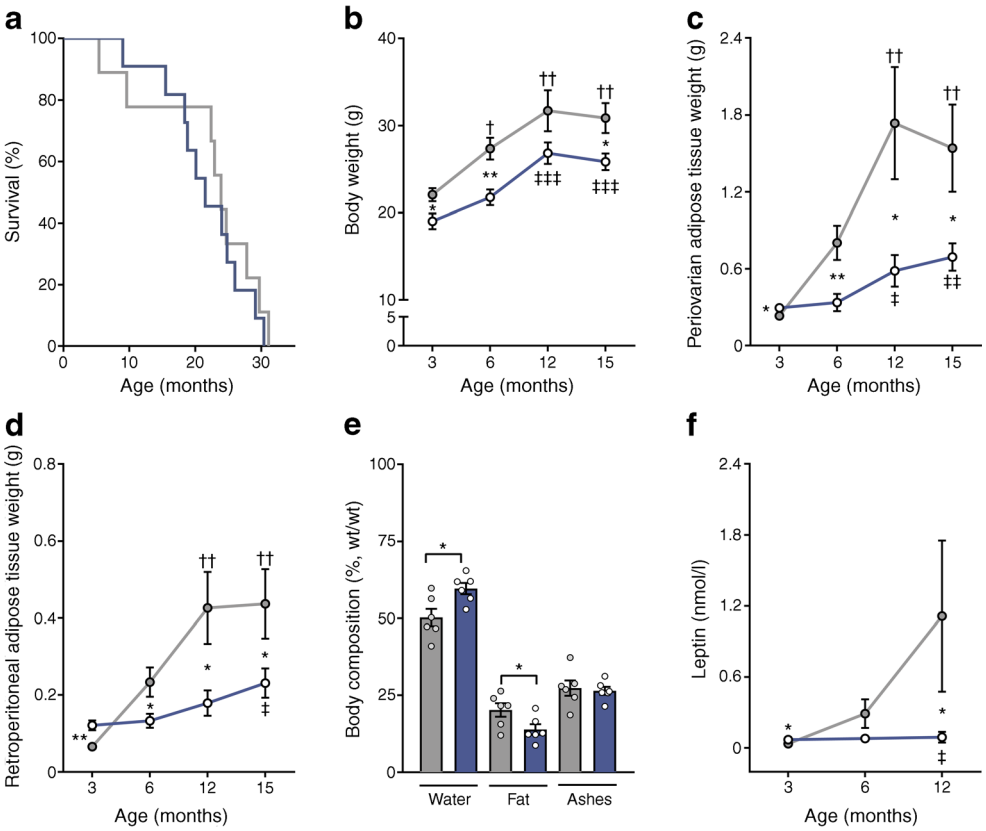

Fig. 1 *Ptn*$^{-/-}$ mice show decreased body weight and reduced adiposity. (**a**) Survival curve, (**b**) body weight, (**c**) periovarian adipose tissue weight, (**d**) retroperitoneal adipose tissue weight, (**e**) body fat and water content analysis, and (**f**) circulating plasma leptin in *Ptn*$^{+/+}$ (grey lines and bars) and *Ptn*$^{-/-}$ (blue lines and bars) female mice. Data are presented as mean ± SEM for $n = 8$ mice/group (**a**–**d**), $n = 6$ mice/group (**e**) and $n = 5$ mice/group (**f**). $^{\dagger}p < 0.05$, $^{\dagger\dagger}p < 0.01$ for differences in the effect of ageing in *Ptn*$^{+/+}$ female mice (vs 3 months); $^{\ddagger}p < 0.05$, $^{\ddagger\ddagger}p < 0.01$, $^{\ddagger\ddagger\ddagger}p < 0.001$ for differences in the effect of ageing in *Ptn*$^{-/-}$ female mice (vs 3 months). $^{*}p < 0.05$; $^{**}p < 0.01$ for differences between *Ptn*$^{-/-}$ and *Ptn*$^{+/+}$ mice

periovarian and retroperitoneal adipose tissue were significantly higher in young *Ptn*$^{-/-}$ mice, whereas in older mice the weight of both fat depots was significantly lower in *Ptn*$^{-/-}$ mice. This pointed to a switch in fat distribution by deletion of *Ptn*, which evolved from a higher degree of adiposity in young animals to a slimness in older mice. Analysis of total body composition in a subset of 6-month-old mice corroborated these data. *Ptn*$^{-/-}$ mice showed a significant reduction in total body fat (20.2% in *Ptn*$^{+/+}$ vs 13.9% in *Ptn*$^{-/-}$ mice), while water content was increased, compared with wild-type controls (Fig. 1e).

Increased adiposity observed in young *Ptn*$^{-/-}$ mice paralleled higher leptin levels when compared with age-matched controls (Fig. 1f). Moreover, *Ptn*$^{+/+}$ mice exhibited an age-related hyperleptinaemia, while circulating leptin in *Ptn*$^{-/-}$ animals did not increase with age compared with their wild-type counterparts, which can be explained by their reduced adiposity.

Altered circulating lipid profile, impaired glucose tolerance and insulin resistance are age-related phenomena in *Ptn*$^{-/-}$ mice Energy imbalance and altered adiposity are related to deteriorated lipid and glucose homeostasis. Accordingly, *Ptn*$^{-/-}$ mice showed lower plasma triacylglycerol levels from 6 to 15 months of age than *Ptn*$^{+/+}$ controls (Fig. 2a), and circulating plasma NEFA were also significantly lower in 15-month-old *Ptn*$^{-/-}$ mice (Fig. 2b). *Ptn*$^{-/-}$ mice exhibited an altered lipid profile, with their plasma triacylglycerol and NEFA concentrations not increasing with age, as happens physiologically in *Ptn*$^{+/+}$ mice.

Next, we explored the impact of *Ptn* deficiency on glucose homeostasis. Although fasting plasma glucose was similar in both groups (Fig. 2c), we found a switch of plasma insulin in *Ptn*$^{-/-}$ mice, departing from lower insulin levels in young mice to hyperinsulinaemia in 15-month-old animals (Fig. 2d).

GTTs and estimated insulin sensitivity did not reveal any differences in the AUC for glucose at 3 and 6 months of age (Fig. 2e). At 9, 12 and 15 months, however, the AUC for glucose was significantly higher in *Ptn*$^{-/-}$ than in *Ptn*$^{+/+}$ mice, indicating a deterioration of glucose tolerance in *Ptn*-deficient animals with age. Furthermore, 15-month-old *Ptn*$^{-/-}$ mice showed a significantly lower QUICKI value than *Ptn*$^{+/+}$ control mice (Fig. 2f), suggesting impaired insulin sensitivity in later life.

Deletion of *Ptn* is associated with differential expression of genes involved in lipid and glucose metabolism in visceral adipose tissue For gene expression analysis, we focused on periovarian adipose tissue. Compared with wild-type controls, 3-month-old *Ptn*$^{-/-}$ mice showed a downregulation of mRNA of the *Ppar-γ* isoforms 1 and 2 (Fig. 3a, b) and their cofactor, *Pgc1-α* (Fig. 3c). Although the expression of these genes

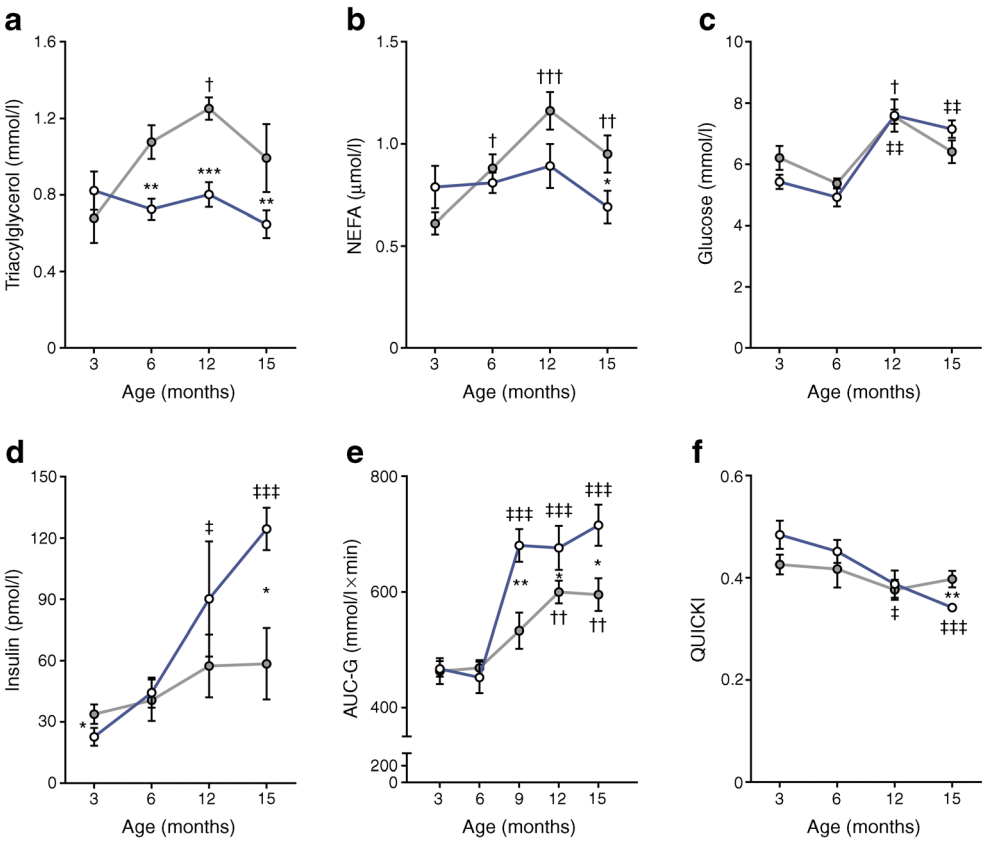

Fig. 2 Altered lipid profiles, impaired glucose tolerance and insulin resistance are age-related phenomena in *Ptn*$^{-/-}$ mice. Plasma biochemistry and insulin sensitivity indexes in *Ptn*$^{+/+}$ female mice (grey lines) and *Ptn*$^{-/-}$ (blue lines) female mice at 3, 6, 12 and 15 months of age. (**a**) Triacylglycerol, (**b**) NEFA, (**c**) glucose, (**d**) insulin, (**e**) AUC for glucose (AUC-G) and (**f**) QUICKI. AUC-G represents the AUC for glucose during the intraperitoneal GTT in female mice fasted for 6 h. Data are mean ± SEM of $n = 8$ mice/group. $^{\dagger}p < 0.05$, $^{\dagger\dagger}p < 0.01$ for differences in the effect of ageing in *Ptn*$^{+/+}$ female mice (vs 3 months); $^{\ddagger}p < 0.05$, $^{\ddagger\ddagger}p < 0.01$, $^{\ddagger\ddagger\ddagger}p < 0.001$ for differences in the effect of ageing in *Ptn*$^{-/-}$ female mice (vs 3 months). $^{*}p < 0.05$; $^{**}p < 0.01$ for differences between *Ptn*$^{-/-}$ and *Ptn*$^{+/+}$ mice

decreased with age in both genotypes (at 12 vs 3 months), the age-related decrease in expression was less pronounced in $Ptn^{-/-}$ mice. These results suggest that the observed $Ptn^{-/-}$ phenotype may be a consequence of defective *Ppar-γ* activation, causing impaired lipid and glucose homeostasis.

To corroborate this notion, we analysed two pivotal peroxisome proliferator-activated receptor (PPAR)-regulated genes, *Lpl* and *Glut-4* (also known as *Slc2a4*), that control lipid and glucose metabolism in white adipocytes. In 3-month-old mice, expression of *Lpl* was significantly lower in $Ptn^{-/-}$ animals than in age-matched controls (Fig. 3d, e). Although both genotypes exhibited an age-related downregulation of *Lpl* and *Glut-4*, the reduced expression was more pronounced in $Ptn^{-/-}$ mice. Thus, both *Ptn* deletion and ageing can cause downregulation of these genes to a similar extent, which is paralleled by changes in $Ppar\text{-}\gamma_1$ and $Ppar\text{-}\gamma_2$ mRNA. In fact, we found a significant positive correlation of the expression of *Lpl* and *Glut-4* with that of $Ppar\text{-}\gamma_1$ and $Ppar\text{-}\gamma_2$ ($p < 0.001$ for all Pearson coefficients).

As these changes may be related to an altered cellular energy balance, we investigated the mRNA levels of *Cpt1α* (also known as *Cpt1a*) and *Ucp-2* in periovarian adipose tissue. We found that *Cpt1α* expression was downregulated by *Ptn* deletion in 3-month-old mice, whereas *Ucp-2* was upregulated (Fig. 3f, g). Although ageing was accompanied by a decrease in *Cpt1α* and an increase in *Ucp-2* expression in $Ptn^{+/+}$ animals, we found no change in $Ptn^{-/-}$ mice (Fig. 3f, g). Analysis of mRNA of genes related to lipid mobilisation, such as β_3-adrenoceptor (*Adr-β*$_3$, also known as *Adrb3*), revealed a decreased expression of this receptor in the periovarian adipose tissue of young $Ptn^{-/-}$ animals compared with wild-type controls (Fig. 3h). Interestingly, in $Ptn^{-/-}$ mice, ageing was accompanied by a significant increase in β_3-adrenoceptor mRNA, whereas in wild-type controls expression of this receptor decreased with age.

All these changes may be related to a state of low-grade inflammation affecting visceral adipocytes, which is caused by the absence of *Ptn*. Indeed, mRNA expression of *Tnf-α* (also known as *Tnf*) was increased in adipocytes from 3-month-old $Ptn^{-/-}$ mice (Fig. 3i). In wild-type animals, ageing was accompanied by increased *Tnf-α* expression, but no changes were observed in $Ptn^{-/-}$ mice.

Genetic inactivation of *Ptn* affects adipocyte size and β-adrenergic-stimulated lipolysis We found a significant decrease of adipocyte size in periovarian adipose tissue of 15-month-old $Ptn^{-/-}$ mice compared with $Ptn^{+/+}$ controls (Fig. 4a, b). To further characterise the alteration of adipose tissue by *Ptn* deletion, catecholamine-stimulated lipolysis was analysed in isolated periovarian adipocytes. Basal lipolysis was significantly lower, and the lipolytic response to isoprenaline significantly higher, in isolated $Ptn^{-/-}$ adipocytes (Fig. 4c). Furthermore, maximum inhibitory actions of insulin on catecholamine-induced lipolysis were significantly lower in $Ptn^{-/-}$ adipocytes compared with wild-type cells (Fig. 4d).

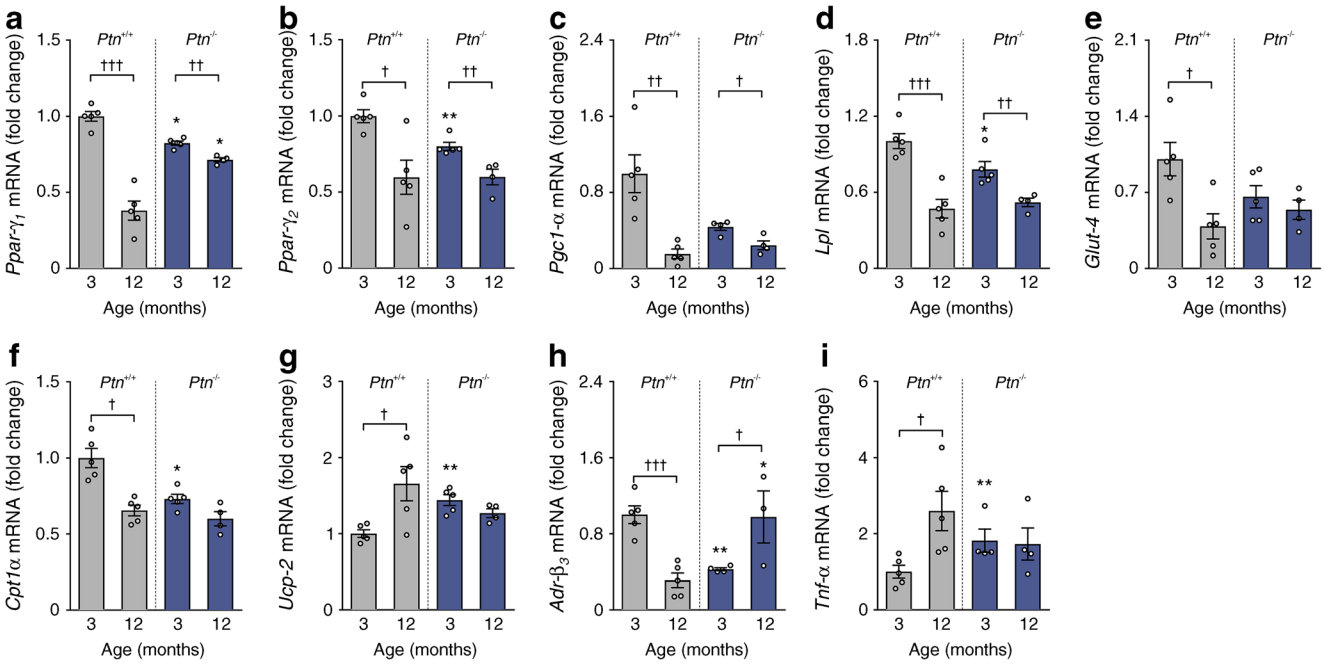

Fig. 3 Deletion of *Ptn* is associated with differential expression of genes involved in lipid and glucose metabolism in periovarian adipose tissue. qPCR analyses of (**a**) *Ppar-γ*$_1$, (**b**) *Ppar-γ*$_2$, (**c**) *Pgc1-α*, (**d**) *Lpl*, (**e**) *Glut-4*, (**f**) *Cpt1α*, (**g**) *Ucp-2*, (**h**) *Adr-β*$_3$ and (**i**) *Tnf-α* in periovarian adipose tissue of 3- and 12-month-old $Ptn^{+/+}$ (grey bars) and $Ptn^{-/-}$ (blue bars) female mice. Data are mean ± SEM of $n = 5$ mice/group, except for 12-month-old $Ptn^{-/-}$ mice ($n = 4$). $^{*}p < 0.05$, $^{**}p < 0.01$ vs $Ptn^{+/+}$ mice of the same age. $^{\dagger}p < 0.05$, $^{\dagger\dagger}p < 0.01$, $^{\dagger\dagger\dagger}p < 0.001$ for differences in the effect of ageing in $Ptn^{+/+}$ (12 vs 3 months)

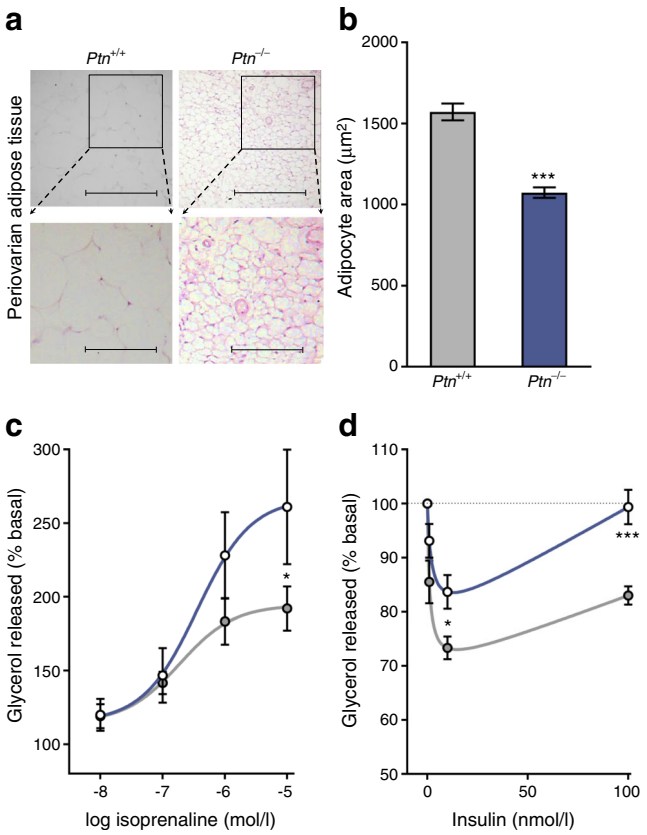

Fig. 4 Genetic inactivation of *Ptn* affects adipocyte size and lipolytic activity after β-adrenergic agonist stimulation. (**a**) Haematoxylin and eosin staining of formalin-fixed periovarian adipose tissue cryosections; ×10 for top panels (scale bar, 200 μm); ×20 for enlargements below (scale bar 100 μm). (**b**) Quantification of periovarian adipocyte cell surface area ($n = 850$ cells for $Ptn^{+/+}$ and 1160 for $Ptn^{-/-}$ mice). (**c**) Concentration–response curves of isoprenaline-stimulated lipolysis in isolated adipocytes from 15-month-old $Ptn^{+/+}$ and $Ptn^{-/-}$ female mice. Data represent lipolytic activities normalised in each experiment to the lipolytic activity in the absence of isoprenaline (basal). Basal lipolysis was 30.7 ± 5.0 and 16.6 ± 2.0 nmol glycerol/mg lipid for $Ptn^{+/+}$ and $Ptn^{-/-}$, respectively ($p < 0.05$). E_{max} (%) was 189.1 ± 16.8 and 273.2 ± 43.3 for $Ptn^{+/+}$ and $Ptn^{-/-}$, respectively ($p < 0.05$). EC_{50} was 81.1 ± 28.3 and 407.8 ± 145.8 nmol/l for $Ptn^{+/+}$ and $Ptn^{-/-}$, respectively ($p < 0.05$). (**d**) Concentration-dependent inhibition of isoprenaline-induced lipolysis by insulin in isolated adipocytes from 15-month-old $Ptn^{+/+}$ and $Ptn^{-/-}$ female mice. Data represent lipolytic activities normalised in each experiment to the lipolytic value in the absence of insulin (control). I_{max} (%) was 26.7 ± 2.1 and 16.3 ± 3.1 for $Ptn^{+/+}$ and $Ptn^{-/-}$, respectively ($p < 0.05$). IC_{50} was 1.47 ± 0.5 and 0.97 ± 0.4 nmol/l for $Ptn^{+/+}$ and $Ptn^{-/-}$. Grey lines and bars, $Ptn^{+/+}$ mice; blue lines and bars, $Ptn^{-/-}$ mice, throughout. (**c**, **d**) Data are mean ± SEM of $n = 7$ mice/group. *$p < 0.05$, ***$p < 0.001$ for differences between $Ptn^{-/-}$ and $Ptn^{+/+}$ mice

Metabolic activity under standard and thermoneutral conditions, and BAT activity in *Ptn*$^{-/-}$ mice The effect of *Ptn* deletion on whole-body metabolic activity at 24°C was monitored in metabolic cages in 6-month-old female mice for 3 days, and subsequently for 7 days under thermoneutrality (30°C). $Ptn^{+/+}$ mice were more active than $Ptn^{-/-}$ mice during the light and dark phases (Fig. 5a), while no differences were observed in total EE in any housing conditions (Fig. 5b). When we calculated the contribution of cold-induced thermogenesis to EE, we found that, at 24°C, the fractions of EE corresponding to cold-induced thermogenesis were higher in $Ptn^{-/-}$ mice than in control animals, both in the light (50.8 ± 3.5% in $Ptn^{-/-}$ vs 39.8 ± 2.1% in $Ptn^{+/+}$ mice, $p < 0.05$) and in the dark phase (35.9 ± 1.9% in $Ptn^{-/-}$ vs 27.1 ± 2.3% in $Ptn^{+/+}$ mice, $p < 0.05$), with a mean daily contribution of thermogenesis to EE of 42.6% and 33.6% for $Ptn^{-/-}$ and $Ptn^{+/+}$ mice, respectively. These differences disappeared when the animals were housed at thermoneutrality.

Analysis of food intake at 24°C and 30°C did not reveal any statistically significant differences between phenotypes (Fig. 5c). We found, however, that the RER at 24°C was lower in $Ptn^{-/-}$ than in $Ptn^{+/+}$ mice (Fig. 5d). The analysis of the maximal and minimal RER shows that $Ptn^{+/+}$ mice consumed carbohydrates as the main source of fuel during the dark period, and a combination of glucose and fatty acids during the light period. $Ptn^{-/-}$ mice were already consuming fatty acids during the dark period, and consumption increased during the light period, indicating that deletion of *Ptn* increases the use of fatty acids for energy production. In thermoneutral conditions, no differences were found in RER between genotypes during either the dark or the light period (Fig. 5d).

After 7 days housed under thermoneutrality, no significant differences were found in the weight of either the retroperitoneal adipose tissue (0.137 ± 0.013 g for $Ptn^{+/+}$ vs 0.189 ± 0.018 g for $Ptn^{-/-}$ mice) or the periovarian adipose tissue (0.279 ± 0.028 g in $Ptn^{+/+}$ vs 0.429 ± 0.134 g in $Ptn^{-/-}$ mice). Moreover, thermoneutrality also reverted the altered lipid profile in $Ptn^{-/-}$ 6-month-old mice. In this condition, no differences were found in circulating triacylglycerols (1.48 ± 0.23 mmol/l in $Ptn^{+/+}$ vs 1.24 ± 0.21 mmol/l in $Ptn^{-/-}$ mice), and the levels of circulating NEFA were even higher in $Ptn^{-/-}$ mice (1.70 ± 0.05 μmol/l) than in $Ptn^{+/+}$ animals (1.48 ± 0.16 μmol/l, $p < 0.05$).

To further assess altered thermogenic function in $Ptn^{-/-}$ mice, thyroid hormones and BAT activity were analysed in 6-month-old female mice. Body temperature was significantly higher (Fig. 6a) and plasma free T_4 lower (Fig. 6b) in $Ptn^{-/-}$ than $Ptn^{+/+}$ mice. An analysis of thyroid hormones in BAT revealed similar T_4 levels in the two groups (Fig. 6c), whereas T_3 concentration (Fig. 6d) was significantly higher in $Ptn^{-/-}$ mice; this was paralleled by an increased activity and expression in BAT of DIO2, the enzyme responsible for tissue T_3 synthesis (Fig. 6e, f). Moreover, expression of mitochondrial UCP-1, responsible for facultative thermogenesis, was increased in the BAT of $Ptn^{-/-}$ mice (Fig. 6g).

Effect of *PTN* in brown adipocyte differentiation We further analysed *Ptn* mRNA during the differentiation of mBAs in vitro. At day 3, we found a tenfold reduction of *Ptn* expression compared with undifferentiated cells; this persisted until day 6, when the cells were fully differentiated (Fig. 7a).

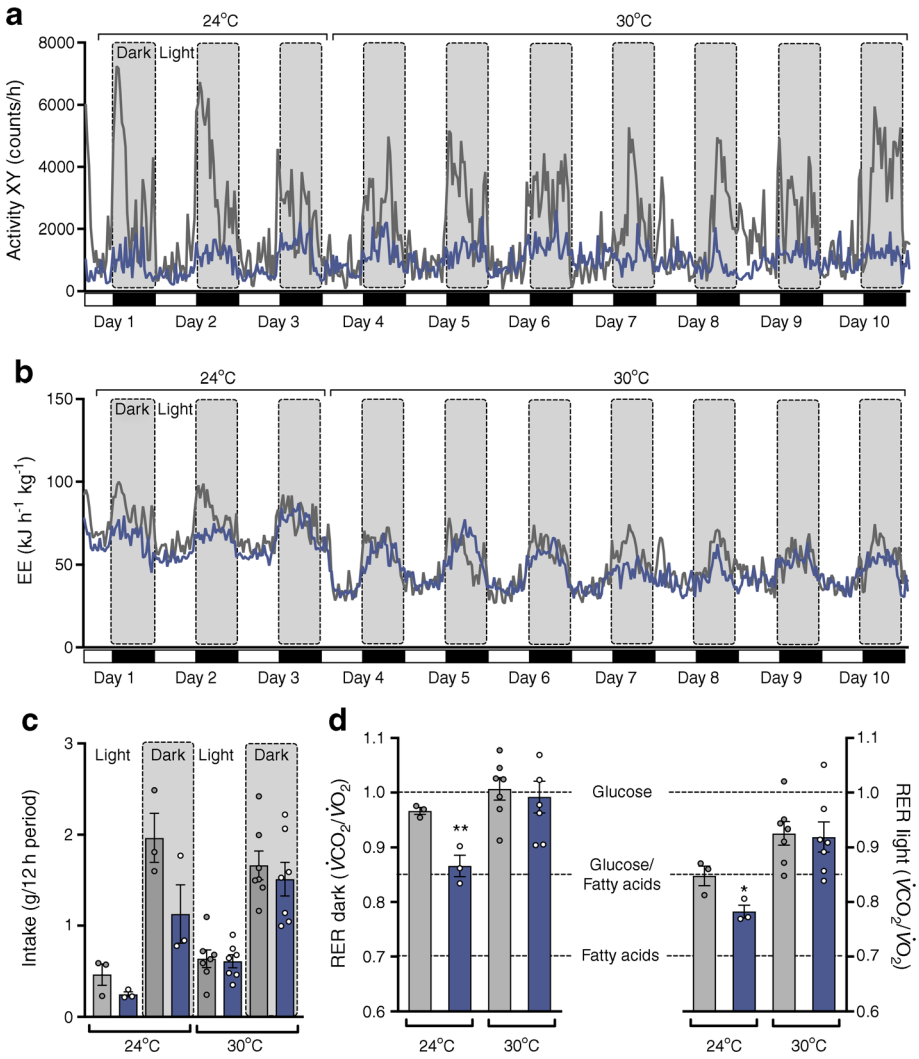

Fig. 5 Altered metabolic activity under standard and thermoneutral conditions with *Ptn* deletion. (**a**) Physical activity in the X and Y axes, (activity XY) and (**b**) EE during the light and dark cycle in 6-month old $Ptn^{+/+}$ and $Ptn^{-/-}$ female mice housed for 3 days at 24°C and 7 days at 30°C. (**c**) Food intake during the dark and light periods and (**d**) RER during the dark and light cycles. Grey lines and bars, $Ptn^{+/+}$ mice; blue lines and bars, $Ptn^{-/-}$ mice. Data are mean ± SEM of the daily intake (3 days at 24°C and 7 days at 30°C) of four mice/group. $^{*}p < 0.05$, $^{**}p < 0.01$ vs $Ptn^{+/+}$ mice at the same temperature

Treatment of mBAs with rPTN during differentiation had no effect on the expression of endogenous *Ptn* (Fig. 7b). PTN supplementation, however, significantly decreased the expression of the mBA markers *Cidea* (20% reduction), *Prdm16* (21% reduction) and *Pgc1-α* (11% reduction) (Fig. 7c–e), reflecting the inhibitory role of PTN in the differentiation of mBAs.

Discussion

Major causes of the high prevalence of metabolic disorders are imbalanced energy metabolism, deranged hormone biology and impaired adipocyte turnover. The characterisation of new targets for the modulation of energy metabolism is of particular interest for the treatment and prevention of metabolic disorders. Here, we provide novel insights into the adipose tissue-specific actions of PTN as a key player in the regulation of energy homeostasis and insulin sensitivity.

We show that *Ptn* deletion modulates adiposity and fat distribution through adipose tissue lipolytic activity and gene expression. $Ptn^{-/-}$-deficient mice had altered body weight and metabolic activity, and their age-related increase in body weight was significantly reduced compared with wild-type animals. Although *Ptn* deletion in 3-month-old mice was associated with a slight increase in visceral adipose tissue depots, the age-related increase in adiposity was significantly reduced in $Ptn^{-/-}$ mice, suggesting a deterioration in adipose tissue expandability, which was further supported by analysis of the total fat mass.

Furthermore, we found alterations in adipocyte cell size and turnover, which are important factors for the development of obesity and metabolic disorders. In fact, in 15-month-old mice, adipocytes from periovarian adipose tissue were smaller in $Ptn^{-/-}$ than in wild-type mice, and this was accompanied by an increase in catecholamine-induced lipolysis. Interestingly, in 12-month-old mice, β_3-adrenoceptor expression paralleled the catecholamine-activated lipolytic activity of the tissue, being significantly higher in the periovarian adipose tissue of $Ptn^{-/-}$

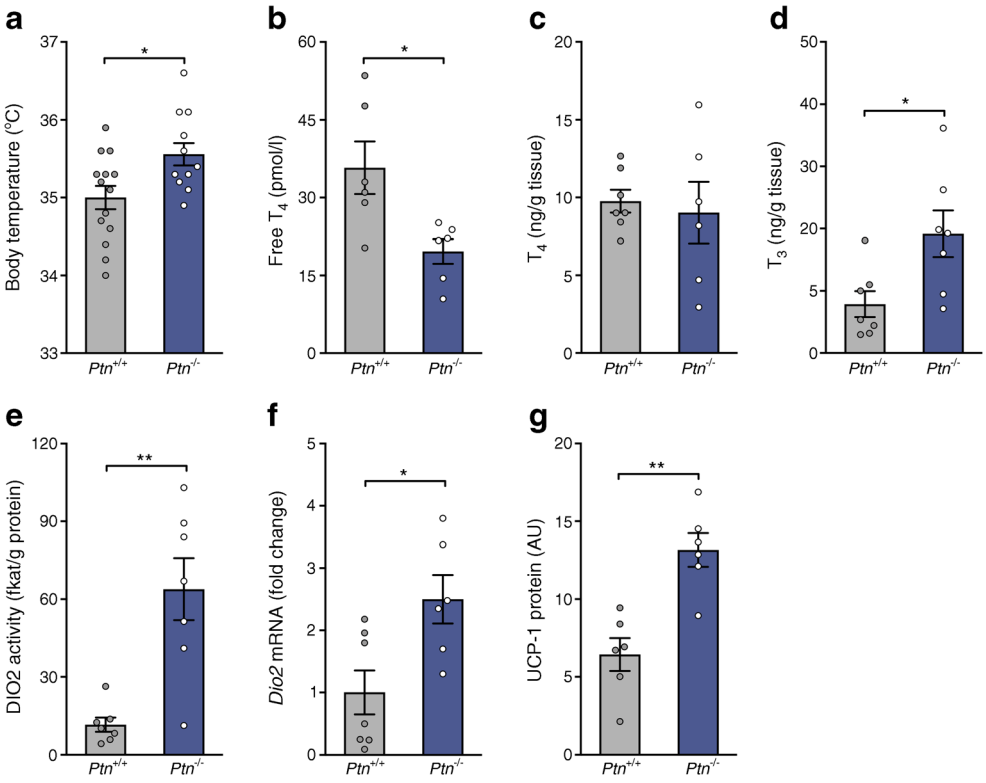

Fig. 6 Genetic inactivation of *Ptn* is associated with impaired thyroid hormones and BAT activity in 6-month old mice. (**a**) Body temperature. (**b**) Plasma concentration of free T_4. Concentration of (**c**) T_4 and (**d**) T_3 in BAT. DIO2 (**e**) activity and (**f**) mRNA expression in BAT. (**g**) UCP-1 in BAT; AU, arbitrary units. Grey bars, $Ptn^{+/+}$ female mice; blue bars, $Ptn^{-/-}$ female mice. Data are mean ± SEM of $n = 14$ and $n = 12$ mice/group (**a**), $n = 7$ mice/group (**c**–**f**) and $n = 6$ mice/group (**b**, **g**). $^{*}p < 0.05$, $^{**}p < 0.01$ for differences between $Ptn^{-/-}$ and $Ptn^{+/+}$ mice

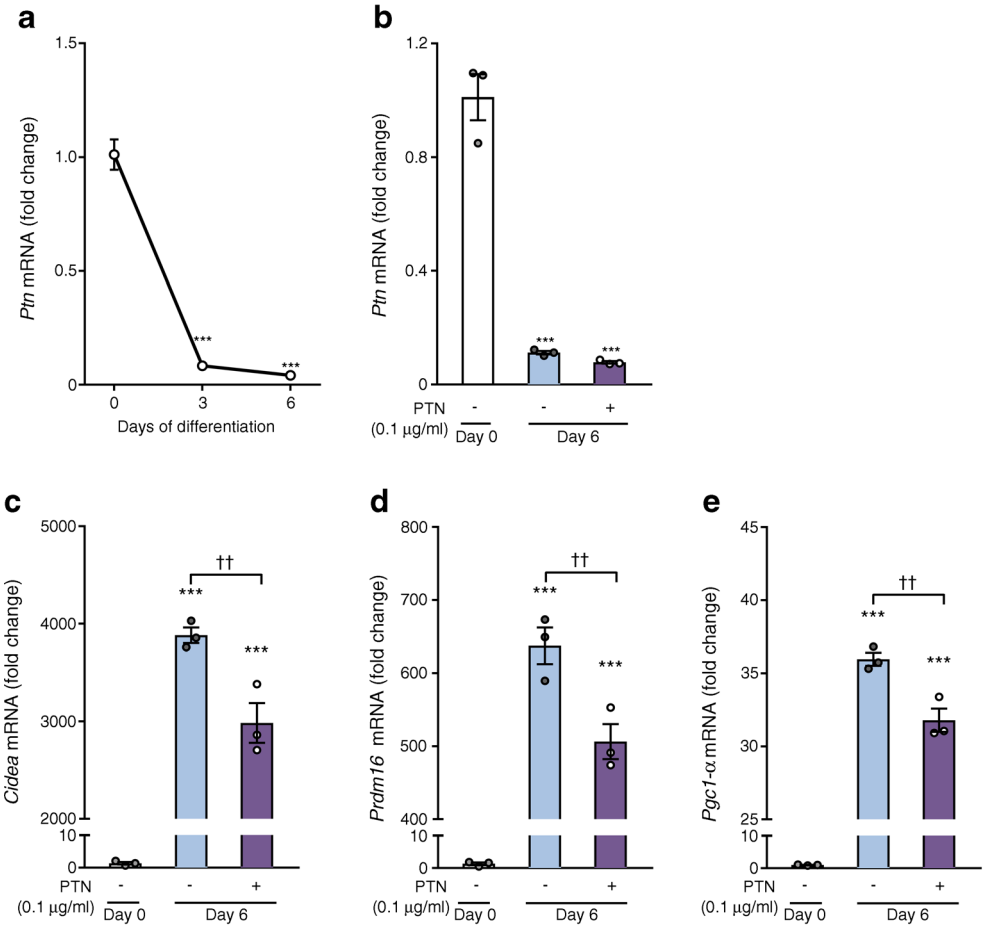

Fig. 7 Effect of PTN in mBA differentiation. (**a**) *Ptn* expression during differentiation of brown pre-adipocyte tissue in mice. qPCR analyses of (**b**) *Ptn* (**c**) *Cidea* (**d**) *Prdm16* and (**e**) *Pgc1-α* expression in undifferentiated pre-adipocytes (day 0, white bars) and differentiated adipocytes (day 6) in either the absence (blue bars) or presence (purple bars) of 0.1 µg/ml PTN. Data are mean ± SEM of $n = 3$ experiments performed in duplicate. $^{***}p < 0.001$ vs undifferentiated (day 0) adipocytes. $^{††}p < 0.01$ for differences in the effect of PTN on differentiation

mice than in wild-type controls. Thus, the increased flux into the circulation of fatty acids and glycerol, released from adipose tissue in response to increased adrenergic stimulation of lipolysis, may account for the increased de novo synthesis of glucose and impaired glucose tolerance in *Ptn*$^{-/-}$ mice.

Importantly, the inhibitory response to insulin of catecholamine-stimulated lipolysis in *Ptn*-deficient periovarian adipocytes was significantly lower than in wild-type cells. These results suggest that *Ptn*$^{-/-}$ mice develop insulin resistance and/or an amelioration of insulin sensitivity in later life, which is accompanied by higher lipolytic activity and an inability to accumulate fat in white adipose tissue.

As evidenced by increased *Tnf*-α expression, the periovarian adipose tissue of *Ptn*$^{-/-}$ mice already exhibits low-grade inflammation at 3 months of age. *Tnf*-α is a well-known inducer of insulin resistance [27], and locally produced *Tnf*-α may act within adipose tissue as a potent autocrine and paracrine regulator of diverse metabolic processes [28]. Indeed, *Ptn* deficiency was associated with decreased *Ppar*-γ_1 and *Ppar*-γ_2 expression in the adipose tissue of young mice. Although rPTN was found to decrease *Ppar*-γ_2 expression in vitro, the same study shows that in vivo injection of a PTN-neutralising antibody slightly decreased *Ppar*-γ_2 levels in adipose tissue [17].

PPAR-γ is essential for adipocyte function, regulating target genes involved in lipid and glucose homeostasis [29]. In particular, PPAR-γ_2 prevents peripheral lipotoxicity, promoting adipose tissue expansion and increasing the lipid-buffering capacity of the peripheral organs [30]. Deletion of *Ppar*-γ_2 in obese mouse models reduces adipose tissue expandability, which is associated with severe insulin resistance [31]. Moreover, *Smad3* knockout mice that have reduced expression of *Ppar*-γ_2 also show impaired adipogenesis and altered lipid accumulation, caused by a decrease in adipocyte number and size [32]. Here, we show that decreased expression of *Ppar*-γ and of its coactivator, *Pgc1*-α, in periovarian adipose tissue is associated with PTN deficiency and may thus play a crucial role in the reduced visceral adiposity, the phenotypic hallmark of the *Ptn* knockout mouse model (Fig. 8).

Remarkably, the expression of *Lpl*, regulated by PPAR-γ, was also downregulated in the periovarian adipose tissue of young *Ptn*$^{-/-}$ *mice*; in these animals, *Cpt1*α mRNA was reduced, whereas *Ucp-2* mRNA was increased to levels similar to those found in 12-month-old *Ptn*$^{+/+}$ mice. Since *Tnf*-α has been proposed to play a role in the upregulation of *Ucp-2* in broadly distributed tissues including BAT, white adipose tissue and skeletal muscle [33], it is tempting to speculate that deletion of *Ptn* may be associated with increased inflammation in periovarian adipose tissue, accelerating the age-related alterations in lipid and glucose metabolism, including insulin resistance and a decreased capacity to store lipids (Fig. 8).

We next explored whether *Ptn* deficiency was associated with the development of whole-body impaired glucose tolerance and insulin resistance. Plasma glucose was similar between groups, suggesting that *Ptn* deletion does not have any impact on glucose homeostasis. There is evidence, however, that impaired glucose tolerance and insulin resistance may develop under normoglycaemia as a consequence of altered lipid metabolism [34, 35]. In fact, although glucose tolerance and insulin responsiveness were higher in the young 3-month-old *Ptn*$^{-/-}$ mice, both variables were clearly impaired with ageing, suggesting that *Ptn* deletion could favour a prediabetic state rendering these animals more prone to developing diabetes mellitus later in life.

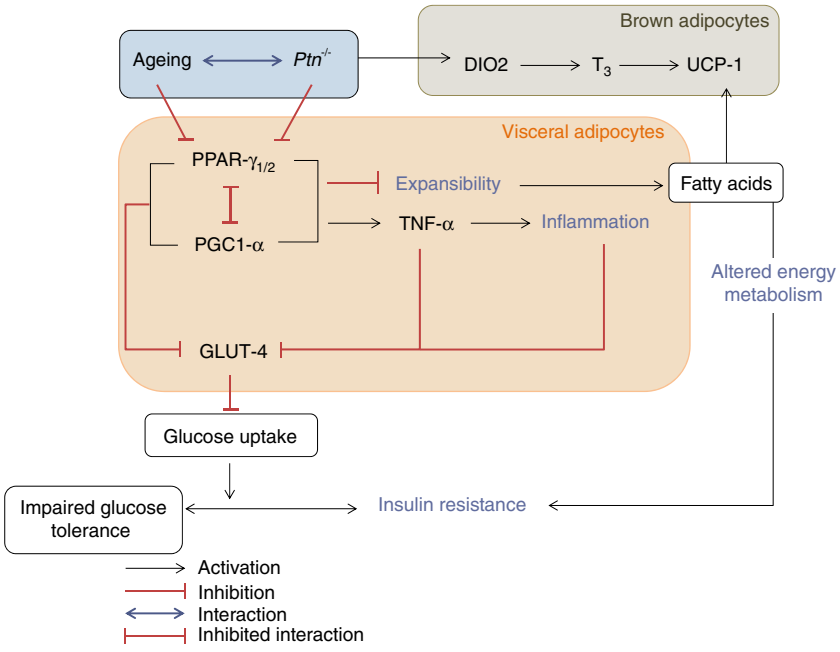

Fig. 8 Summary of the molecular mechanisms by which PTN deficiency alters the dynamics of adipose lipid turnover and impairs energy metabolism. PGC1-α, peroxisome proliferator-activated receptor γ coactivator 1-α

We further explored energy homeostasis in the $Ptn^{-/-}$ model and found that $Ptn^{-/-}$ mice consumed a combination of glucose and fatty acids during the dark period and further increased this consumption during the light period, pointing to an augmented energy production from fatty acids. The main oxidative tissue in which fatty acids are used as energy substrates by β-oxidation is skeletal muscle [36]. However, $Ptn^{-/-}$ mice exhibited reduced physical activity, suggesting that fatty acids may be redirected for oxidation in other tissues. In fact, the fraction of EE that accounts for cold-induced thermogenesis was significantly higher in $Ptn^{-/-}$ than $Ptn^{+/+}$ mice. These results are in good agreement with previous studies showing that, at 22–24°C, mice require over one third of their EE to maintain core body temperature [22]. Since, in $Ptn^{-/-}$ mice, cold-induced thermogenesis represents more than 40% of EE, we looked at alterations in BAT, the tissue accounting for the production of heat by facultative thermogenesis. Brown fat thermogenesis depends on fatty acid utilisation provided by endogenous lipolysis, the mitochondrial machinery involved in fatty translocation and oxidation, and the uncoupling of ATP synthesis by UCP-1. In this regard, we found higher UCP-1 levels in the BAT of $Ptn^{-/-}$ than wild-type mice. Expression and activation of UCP-1 is regulated by fatty acids, cold exposure or noradrenaline (norepinephrine), and T_3 is able to increase this stimulation by noradrenaline [37]. Subsequently, the conversion of T_4 to T_3 by DIO2 is required for the thermogenic function of BAT [38]. Analysis of BAT revealed increased DIO2 activity and expression, together with higher concentrations of T_3 in BAT of $Ptn^{-/-}$ mice. Interestingly, these mice also had lower levels of plasma free T_4. Thus, in BAT, *Ptn* deletion may be associated with an increased conversion of T_4 to T_3 by DIO2, accounting for the increased UCP-1 production and the ensuing elevation of body temperature. This process can be maintained by an increased oxidation of fatty acids as energy substrates, made available from an increased lipolytic activity of adipose tissue despite sufficient glucose availability. Such a preferential oxidation of fatty acids may contribute to the diminished plasma concentration of fatty acids and triacylglycerols, as well as to the reduced adiposity observed in the periovarian and retroperitoneal adipose tissue of $Ptn^{-/-}$ mice.

Further exploring the mechanism of altered thermogenesis in $Ptn^{-/-}$ mice, we found that the differentiation of brown preadipocytes (mBAs) blunted *Ptn* expression, and that treatment of mBAs with rPTN diminished the expression of brown fat markers (*Cidea*, *Prdm16* and *Pgc1-α*). Thus, although it is known that *Ptn* expression is suppressed during the differentiation of white adipocytes [16], our results reveal for the first time that BAT differentiation is regulated by changes in *Ptn* expression and suggest an inhibitory role of this cytokine in brown fat differentiation and thermogenesis.

In conclusion, we propose that the lipodystrophic phenotype of $Ptn^{-/-}$ mice is related to enhanced thermogenesis in BAT that is maintained by active lipid mobilisation from white fat. In support of this hypothesis, we found that when housing animals at thermoneutrality, a condition that blunts thermogenesis, the differences in adiposity and circulating triacylglycerols observed at 24°C disappeared, and NEFA concentrations were even higher in $Ptn^{-/-}$ than control mice. These results, together with the increased RER observed at 30°C in $Ptn^{-/-}$ mice, point to a pronounced inhibition of unrestrained lipolysis at thermoneutrality in $Ptn^{-/-}$ mice.

Conclusion

This is the first study demonstrating that PTN expression is essential to preserve the dynamics of adipose lipid turnover and plasticity. In particular, in visceral and brown fat pads, ablation of *Ptn* renders mice more prone to developing insulin resistance and/or an amelioration of insulin sensitivity in later life. These conditions are concomitant with altered expansibility of periovarian adipose tissue and impaired thermogenesis of brown adipose cells. The finding that *Ptn* deficiency and ageing alter the expression profile of a set of genes regulating lipid uptake and utilisation supports the notion that defective PPAR-γ activation accounts for the phenotype of our mouse model, by inducing impairments in lipid and glucose homeostasis (Fig. 8).

Acknowledgements We thank our colleagues in the Animal Facility of the Universidad CEU San Pablo. The immortalised mBAs were kindly supplied by A. M. Valverde (Alberto Sols Biomedical Research Institute [IIBm; CSIC/UAM], Madrid, Spain).

Data availability The datasets generated during and/or analysed during the current study are available from the corresponding author on reasonable request.

Funding This work was supported by the Spanish Ministry of Economy and Competitiveness (SAF2014-56671-R, SAF2012-32491, SAF2010-19603, BFU2013-47384-R and BFU2016-78951-R) and Community of Madrid (S2010/BMD-2423; S2017/BMD-3864).

Duality of interest The authors declare that there is no duality of interest associated with this manuscript.

Contribution statement JS, GM-G, MJO and IV-A performed acquisition, analysis and interpretation of the data, and drafted the manuscript. MGS-A, MC, MA, DH, BZ, ML, JP, EG, MV-R and MV were involved in acquisition, analysis and interpretation of the data. GH and MV analysed and interpreted the data and drafted the manuscript. MPR-A initiated and designed the study, performed analysis and interpretation of the data, and contributed to drafting the manuscript. All authors revised and approved the final version of the manuscript. MPR-A is the guarantor of this work.

References

1. Bohlen P, Kovesdi I (1991) HBNF and MK, members of a novel gene family of heparin-binding proteins with potential roles in embryogenesis and brain function. Prog in Growth Factor Res 3:143–157. https://doi.org/10.1016/S0955-2235(05)80005-5
2. Deuel TF, Zhang N, Yeh HJ, Silos-Santiago I, Wang ZY (2002) Pleiotrophin: a cytokine with diverse functions and a novel signaling pathway. Arch Biochem Biophys 397:162–171. https://doi.org/10.1006/abbi.2001.2705
3. Azizan A, Gaw JU, Govindraj P, Tapp H, Neame PJ (2000) Chondromodulin I and pleiotrophin gene expression in bovine cartilage and epiphysis. Matrix Biol 19:521–531. https://doi.org/10.1016/S0945-053X(00)00110-4
4. Hienola A, Pekkanen M, Raulo E, Vanttola P, Rauvala H (2004) HB-GAM inhibits proliferation and enhances differentiation of neural stem cells. Mol Cell Neurosci 26:75–88. https://doi.org/10.1016/j.mcn.2004.01.018
5. Mitsiadis TA, Salmivirta M, Muramatsu T et al (1995) Expression of the heparin-binding cytokines, midkine (MK) and HB-GAM (pleiotrophin) is associated with epithelial-mesenchymal interactions during fetal development and organogenesis. Development 121:37–51
6. Sakurai H, Bush KT, Nigam SK (2001) Identification of pleiotrophin as a mesenchymal factor involved in ureteric bud branching morphogenesis. Development 128:3283–3293
7. Weng T, Liu L (2010) The role of pleiotrophin and beta-catenin in fetal lung development. Respir Res 11:80. https://doi.org/10.1186/1465-9921-11-80
8. Imai S, Kaksonen M, Raulo E et al (1998) Osteoblast recruitment and bone formation enhanced by cell matrix-associated heparin-binding growth-associated molecule (HB-GAM). J Cell Biol 143:1113–1128. https://doi.org/10.1083/jcb.143.4.1113
9. Vanderwinden JM, Mailleux P, Schiffmann SN, Vanderhaeghen JJ (1992) Cellular distribution of the new growth factor pleiotrophin (HB-GAM) mRNA in developing and adult rat tissues. Anat Embryol 186:387–406
10. Schulte AM, Wellstein A (1997) Pleiotrophin and related molecules. In: Bicknell R, Lewis CE, Ferrara N (eds) Tumour angiogenesis. Oxford University Press, Oxford, pp 273–289
11. Li G, Bunn JR, Mushipe MT, He Q, Chen X (2005) Effects of pleiotrophin (PTN) over-expression on mouse long bone development, fracture healing and bone repair. Calcif Tissue Int 76:299–306. https://doi.org/10.1007/s00223-004-0145-6
12. Petersen W, Wildemann B, Pufe T, Raschke M, Schmidmaier G (2004) The angiogenic peptide pleiotrophin (PTN/HB-GAM) is expressed in fracture healing: an immunohistochemical study in rats. Arch Orthop Trauma Surg 124:603–607. https://doi.org/10.1007/s00402-003-0582-0
13. Kaspiris A, Mikelis C, Heroult M et al (2013) Expression of the growth factor pleiotrophin and its receptor protein tyrosine phosphatase beta/zeta in the serum, cartilage and subchondral bone of patients with osteoarthritis. Joint, bone, spine 80:407–413. https://doi.org/10.1016/j.jbspin.2012.10.024
14. Papadimitriou E, Mikelis C, Lampropoulou E et al (2009) Roles of pleiotrophin in tumor growth and angiogenesis. Eur Cytokine Netw 20:180–190. https://doi.org/10.1684/ecn.2009.0172
15. Yi C, Xie WD, Li F et al (2011) MiR-143 enhances adipogenic differentiation of 3T3-L1 cells through targeting the coding region of mouse pleiotrophin. FEBS Lett 585:3303–3309. https://doi.org/10.1016/j.febslet.2011.09.015
16. Gu D, Yu B, Zhao C et al (2007) The effect of pleiotrophin signaling on adipogenesis. FEBS Lett 581:382–388. https://doi.org/10.1016/j.febslet.2006.12.043
17. Wong JC, Krueger KC, Costa MJ et al (2016) A glucocorticoid- and diet-responsive pathway toggles adipocyte precursor cell activity in vivo. Sci Signal 9:ra103. https://doi.org/10.1126/scisignal.aag0487
18. Amet LE, Lauri SE, Hienola A et al (2001) Enhanced hippocampal long-term potentiation in mice lacking heparin-binding growth-associated molecule. Mol Cell Neurosci 17:1014–1024. https://doi.org/10.1006/mcne.2001.0998
19. Herradon G, Ezquerra L, Nguyen T et al (2004) Pleiotrophin is an important regulator of the renin-angiotensin system in mouse aorta. Biochem Biophys Res Commun 324:1041–1047. https://doi.org/10.1016/j.bbrc.2004.09.161
20. Cacho J, Sevillano J, de Castro J, Herrera E, Ramos MP (2008) Validation of simple indexes to assess insulin sensitivity during pregnancy in Wistar and Sprague-Dawley rats. Am J Phys Endocrinol Metab 295:E1269–E1276. https://doi.org/10.1152/ajpendo.90207.2008
21. Ramos MP, Crespo-Solans MD, del Campo S, Cacho J, Herrera E (2003) Fat accumulation in the rat during early pregnancy is modulated by enhanced insulin responsiveness. Am J Phys Endocrinol Metab 285:E318–E328. https://doi.org/10.1152/ajpendo.00456.2002
22. Abreu-Vieira G, Xiao C, Gavrilova O, Reitman ML (2015) Integration of body temperature into the analysis of energy expenditure in the mouse. Mol Metab 4:461–470. https://doi.org/10.1016/j.molmet.2015.03.001
23. Morreale de Escobar G, Pastor R, Obregon MJ, Escobar del Rey F (1985) Effects of maternal hypothyroidism on the weight and thyroid hormone content of rat embryonic tissues, before and after onset of fetal thyroid function. Endocrinology 117:1890–1900. https://doi.org/10.1210/endo-117-5-1890
24. Obregon MJ, Ruiz de Ona C, Hernandez A, Calvo R, Escobar del Rey F, Morreale de Escobar G (1989) Thyroid hormones and 5′-deiodinase in rat brown adipose tissue during fetal life. Am J Phys 257:E625–E631
25. Valverde AM, Mur C, Brownlee M, Benito M (2004) Susceptibility to apoptosis in insulin-like growth factor-I receptor-deficient brown adipocytes. Mol Biol Cell 15:5101–5117. https://doi.org/10.1091/mbc.e03-11-0853
26. Calderon-Dominguez M, Sebastian D, Fucho R et al (2016) Carnitine palmitoyltransferase 1 increases lipolysis, UCP1 protein expression and mitochondrial activity in brown adipocytes. PLoS One 11:e0159399
27. Kern PA, Ranganathan S, Li C, Wood L, Ranganathan G (2001) Adipose tissue tumor necrosis factor and interleukin-6 expression in human obesity and insulin resistance. Am J Phys Endocrinol Metab 280:E745–E751. https://doi.org/10.1152/ajpendo.2001.280.5.E745
28. Ruan H, Lodish HF (2003) Insulin resistance in adipose tissue: direct and indirect effects of tumor necrosis factor-alpha. Cytokine Growth Factor Rev 14:447–455. https://doi.org/10.1016/S1359-6101(03)00052-2
29. Janani C, Ranjitha Kumari BD (2015) PPAR gamma gene—a review. Diabetes Metab Syndr 9:46–50. https://doi.org/10.1016/j.dsx.2014.09.015
30. Medina-Gomez G, Gray S, Vidal-Puig A (2007) Adipogenesis and lipotoxicity: role of peroxisome proliferator-activated receptor γ (PPARγ) and PPARγcoactivator-1 (PGC1). Public Health Nutr 10:1132–1137. https://doi.org/10.1017/S1368980007000614
31. Medina-Gomez G, Gray SL, Yetukuri L et al (2007) PPAR gamma 2 prevents lipotoxicity by controlling adipose tissue expandability and peripheral lipid metabolism. PLoS Genet 3:e64
32. Tan CK, Leuenberger N, Tan MJ et al (2011) Smad3 deficiency in mice protects against insulin resistance and obesity induced by a high-fat diet. Diabetes 60:464–476. https://doi.org/10.2337/db10-0801

33. Masaki T, Yoshimatsu H, Kakuma T et al (1999) Induction of rat uncoupling protein-2 gene treated with tumour necrosis factor alpha in vivo. Eur J Clin Investig 29:76–82. https://doi.org/10.1046/j.1365-2362.1999.00403.x
34. Lee Y, Hirose H, Ohneda M, Johnson JH, McGarry JD, Unger RH (1994) Beta-cell lipotoxicity in the pathogenesis of non-insulin-dependent diabetes mellitus of obese rats: impairment in adipocyte-beta-cell relationships. Proc Natl Acad Sci U S A 91:10878–10882. https://doi.org/10.1073/pnas.91.23.10878
35. Del Prato S, Enzi G, Vigili de Kreutzenberg S et al (1990) Insulin regulation of glucose and lipid metabolism in massive obesity. Diabetologia 33:228–236. https://doi.org/10.1007/BF00404801
36. Speakman JR (2013) Measuring energy metabolism in the mouse — theoretical, practical, and analytical considerations. Front Physiol 4:34
37. Obregon MJ, Pitamber R, Jacobsson A, Nedergaard J, Cannon B (1987) Euthyroid status is essential for the perinatal increase in thermogenin mRNA in brown adipose tissue of rat pups. Biochem Biophys Res Commun 148:9–14. https://doi.org/10.1016/0006-291X(87)91069-2
38. Bianco AC, Silva JE (1988) Cold exposure rapidly induces virtual saturation of brown adipose tissue nuclear T3 receptors. Am J Phys 255:E496–E503